



## Electrochemical Fabrication of Highly Ordered ZrO<sub>2</sub>-HfO<sub>2</sub> Binary Oxides Nanotube Arrays

LINGJIE LI<sup>1</sup>, JING XU<sup>1</sup>, JINGLEI LEI<sup>1\*</sup>, JIANXIN HE<sup>1</sup>, JIARUI ZHANG<sup>1</sup>, NIANBING LI<sup>2</sup> and SHENGTAO ZHANG<sup>1</sup>

<sup>1</sup>School of Chemistry and Chemical Engineering, Chongqing University, Chongqing, 400044, P.R. China

<sup>2</sup>School of Chemistry and Chemical Engineering, Southwest University, Chongqing, 400715, P.R. China

\*Corresponding author: Fax: +86 23 65112328; Tel: +86 13983064116; E-mail: jllei@cqu.edu.cn

Received: 28 February 2014;

Accepted: 16 May 2014;

Published online: 16 July 2014;

AJC-15599

The present work demonstrates a facile approach to fabricate highly ordered nanotubular ZrO<sub>2</sub>-HfO<sub>2</sub> binary oxides. Zr-Hf alloy was electrochemically anodized in an ethylene glycol electrolyte containing small amounts of fluoride *via* a two-step process. The field emission scanning electron microscopy images show the highly ordered nanotube arrays with a length of approximately 6.8 μm, an average diameter of approximate 32 nm and a tube density of  $3 \times 10^{10}$  cm<sup>-2</sup> were formed on the Zr-Hf alloy surface. X-ray photoelectron spectroscopy analysis provides evidence that the composition of the formed nanotubes is ZrO<sub>2</sub>-HfO<sub>2</sub> binary oxides. X-ray diffraction studies indicates that monoclinic ZrO<sub>2</sub> and HfO<sub>2</sub> with small amount of tetragonal phase ZrO<sub>2</sub> coexist in the nanotubular binary oxides layer after thermal annealing at 400 °C for 3 h. The present electrochemical approach can be extended to prepare the highly ordered nanotubular oxides with a wide range of composition and functionalities.

**Keywords:** Nanotubes, ZrO<sub>2</sub>-HfO<sub>2</sub> binary oxides, Electrochemical anodization, FESEM, XPS, XRD.

### INTRODUCTION

Due to the high thermal and chemical stability, high dielectric constant, improved mechanical strength, catalytic properties and low electrical conductivity, zirconia (zirconium oxide, ZrO<sub>2</sub>) has been widely used as protective coatings, optical films, gas sensors, solid electrolytes, catalysts and catalyst supports<sup>1-6</sup>. Hafnia (hafnium oxide, HfO<sub>2</sub>) has similar crystal structure and ion conductivity with zirconia, but much higher thermal and chemical stability and much lower electrical conductivity<sup>7,8</sup>. Mixing small amount of hafnia into zirconia to form binary ZrO<sub>2</sub>-HfO<sub>2</sub> system can lead to a noticeable enhancement of the properties of ZrO<sub>2</sub> and allow to overcome the high cost problem related to the use of pure Hf oxides<sup>9</sup>. Furthermore, highly ordered nanotubular binary ZrO<sub>2</sub>-HfO<sub>2</sub> materials have much higher surface area, which benefits to drastically improve working efficiency, to induce new functionalities and hence broaden their applications<sup>10,11</sup>. Therefore, binary ZrO<sub>2</sub>-HfO<sub>2</sub> materials with highly ordered nanotubular structure are appealing and the facile methods to fabricate them are desired.

Electrochemical formation technique has been widely used to prepare highly ordered architectures due to the advantages of the simplicity and the unnecessary of vacuum and high temperature. Not only as the usual method to produce porous anodic alumina oxide (AAO) templates<sup>12-14</sup>, electro-

chemical anodization has also been used to fabricate vertically orientated self-organized oxide nanotubes on pure valve metals such as Ti<sup>15-18</sup>, Zr<sup>19-23</sup>, Hf<sup>24,25</sup>, Nb<sup>26,27</sup>, W<sup>28</sup> and *etc*<sup>29</sup>. So far as we know, though a great effort has been made to synthesize ZrO<sub>2</sub> or HfO<sub>2</sub> nanotubes by anodizing of pure Zr or Hf metal in certain electrolytes<sup>19-25</sup>, the fabrication of highly ordered nanotubular binary ZrO<sub>2</sub>-HfO<sub>2</sub> materials by electrochemical anodizing of Zr-Hf alloy has not been reported earlier.

In the present work, the feasibility to fabricate highly ordered nanotubular ZrO<sub>2</sub>-HfO<sub>2</sub> binary oxides by electrochemical anodization is exploited. Zr-Hf alloy is electrochemically anodized in an ethylene glycol electrolyte *via* a two-step process at room temperature. The morphology and composition of the anodized oxide layer is studied, which confirms the successful fabrication of the highly ordered ZrO<sub>2</sub>-HfO<sub>2</sub> binary oxides nanotubue arrays *via* the electrochemical anodization approach.

### EXPERIMENTAL

Zr-Hf binary alloy foils (97.9:2.1 wt. %; 0.2 mm thickness; Yunjie Metal Co., Ltd., P. R. China) were abraded with 200, 800, 2000# grit emery papers, degreased ultrasonically in absolute ethanol for 3 min, chemically etched in a HF/HNO<sub>3</sub>/H<sub>2</sub>O (3:14:5 in mass) solution for 5 s, then rinsed with deionized water and finally dried with air.

The electrochemical anodization experiments were carried out using an electrochemical set-up consisting of a DH1719A-5 potentiost (Beijing Dahua Electronic Co., P.R. China) and a two-electrode arrangement with the pre-treated Zr-Hf binary alloy foil as the working electrode and a stainless steel plate as the counter electrode. The anodization electrolyte was a mixed solution of ethylene glycol (100 mL) and 17.5 wt. %  $\text{NH}_4\text{F}$  aqueous electrolyte (2 mL), which was prepared from analytical grade chemicals and deionized water. The first anodization step was conducted at 30 V for 0.5 h and then the anodic layer formed was removed by ultrasonically soaking in ethanol for 5 min and then peeling away with an adhesive tape. Under the identical conditions, the second anodization step was performed for 20 min, after which the samples were rinsed with deionized water and then dried with air. All the above experiments were conducted at room temperature.

The morphologies of the samples were characterized using a field emission scanning electron microscope (FESEM, FEI Nova 400, Holland). The chemical and phase composition of the samples was analyzed by X-ray photoelectron spectroscopy (XPS, Thermoelectron ESCALAB250, USA) and X-ray diffraction (XRD, X'Pert PRO, PANalytical B.V., Holland), respectively.

## RESULTS AND DISCUSSION

Fig. 1a shows the surface morphology of the oxide layer after the one-step anodization. Many irregular nanopores distribute randomly on the surface, which indicates that the one-step anodization process is insufficient for obtaining well-aligned nanotubular oxide layer. The irregular nanoporous anodic layer was subsequently removed. The corresponding imprints display an ordered hexagonally packed pattern with an average diameter of 40 nm (Fig. 1b). Further information about the imprints arrangement regularity can be derived in virtue of FFTs (the inset in Fig. 1b). Six distinct spots uniformly distribute on each edge of the hexagon, which confirms that the imprints have a regular hexagonal pattern. Fig. 1c and 1d (with the inset), respectively illustrate the top view and cross-sectional view of the anodic oxide layer formed during the second anodization step. The highly regular and ordered nanotube arrays with a length of approximately 6.8  $\mu\text{m}$ , an average diameter of approximate 32 nm and a pore density of  $3 \times 10^{10} \text{ cm}^{-2}$  are grown.

Comparing Fig. 1c and 1d with Fig. 1a, it can be found that the ordered nanotubes grown in the second-step anodization appreciably outperform those fabricated by the one-step anodization in terms of size uniformity and arrangement orderliness, which confirms the necessity of the treatments to induce the imprints with ordered hexagonally packed pattern on the Zr-Hf surface and two-step electrochemical anodization method is a facile approach to fabricate the highly ordered nanotubular architecture.

The composition of the anodic nanotube arrays was investigated by using X-ray photoelectron spectroscopy (XPS). From the survey spectrum, the existence of elements Zr, Hf, O, F and C is confirmed. C, F and small amount of O (shown as peak 1 in Fig. 2d) might come from the anodization electrolyte and/or are contaminations that induced during the

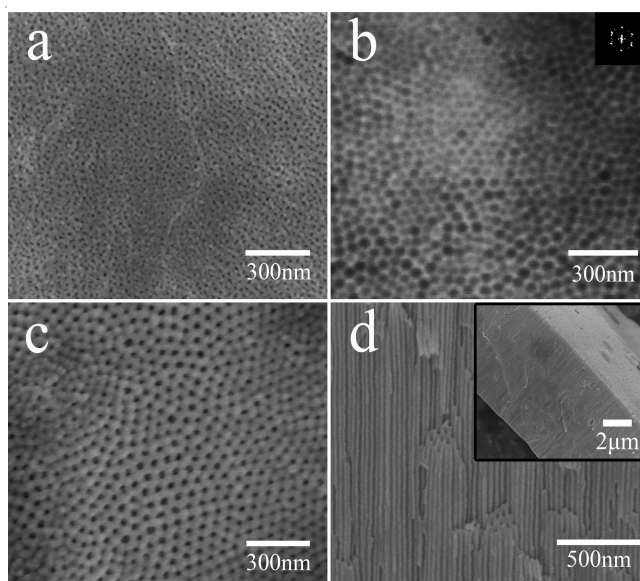


Fig. 1. FE-SEM micrographs of (a) top view of the first-step anodized sample. (b) imprints after removal of the first-step anodized layer (inset: FFTs pattern of the FE-SEM image). (c) top view and (d) cross-sectional view of the two-step anodized sample (inset: low resolution of cross-sectional view)

storage of the sample in air. The high-resolution spectra for the major component elements of the nanotube arrays are shown in Figs. 2 a-d. The Hf4f and O2s peaks are overlapped (Fig. 2a). The deconvoluted Hf4f spectrum is centered at 17.6 eV, which can be attributed to Hf-O bond<sup>30</sup>. Moreover, the formation of  $\text{HfO}_2$  is confirmed by the Hf4d<sub>5/2</sub> spectrum (Fig. 2b). The binding energy (BE) of Hf4d<sub>5/2</sub> has a value of 212.3 eV for the nanotube arrays, which is a little lower than that of bulk  $\text{HfO}_2$ , 213.1 eV<sup>31</sup>. The shift to a slightly lower value may be ascribed to the different chemical environment that  $\text{HfO}_2$  experiences from that in bulk  $\text{HfO}_2$ . Analogous consideration can be extended to the shifted BEs observed in case of Zr3d<sub>5/2</sub>, which is centered at 181.4 eV (Fig. 2c), 0.8 eV lower than that of bulk  $\text{ZrO}_2$ , 182.2 eV<sup>31</sup>. The peak 2 of O1s spectrum (Fig. 2d) can be attributed to  $\text{ZrO}_2$ - $\text{HfO}_2$  binary oxides (M-O).

Quantitative analysis of XPS results reveal that the highly ordered nanotube arrays anodically fabricated on Zr-Hf alloy essentially consists of 25.6 at % Zr, 0.3 at % Hf and 57.3 at % O. According to the peak 2 area of O1s spectrum (Fig. 2d), the atomic fraction of O for  $\text{ZrO}_2$ - $\text{HfO}_2$  binary oxides is calculated as 48.7 at %, which is approximately twice of that of Zr and Hf in the anodic nanotube array layer. Hence, it is inferred that the highly ordered nanotube arrays consists of oxides with stoichiometry of  $\text{ZrO}_2$  and  $\text{HfO}_2$ . Moreover, the molar ratio of  $\text{ZrO}_2$  and  $\text{HfO}_2$  in the anodic layer is approximately equivalent to that of Zr and Hf in the alloy, implying that the ratio of  $\text{ZrO}_2$  and  $\text{HfO}_2$  might be flexibly controlled by adjusting the ratio of Zr and Hf in the alloy.

Fig. 3 illustrates the XRD patterns of the anodized sample after further thermal annealing at 400 °C for 3 h in air. Besides the diffraction peaks of metallic Zr-Hf substrate, some other diffraction peaks are observed, among which the most majority is the monoclinic diffraction peaks. According to JCPDS card No. 37-1484 (monoclinic  $\text{ZrO}_2$ ) and JCPDS card No. 06-0318

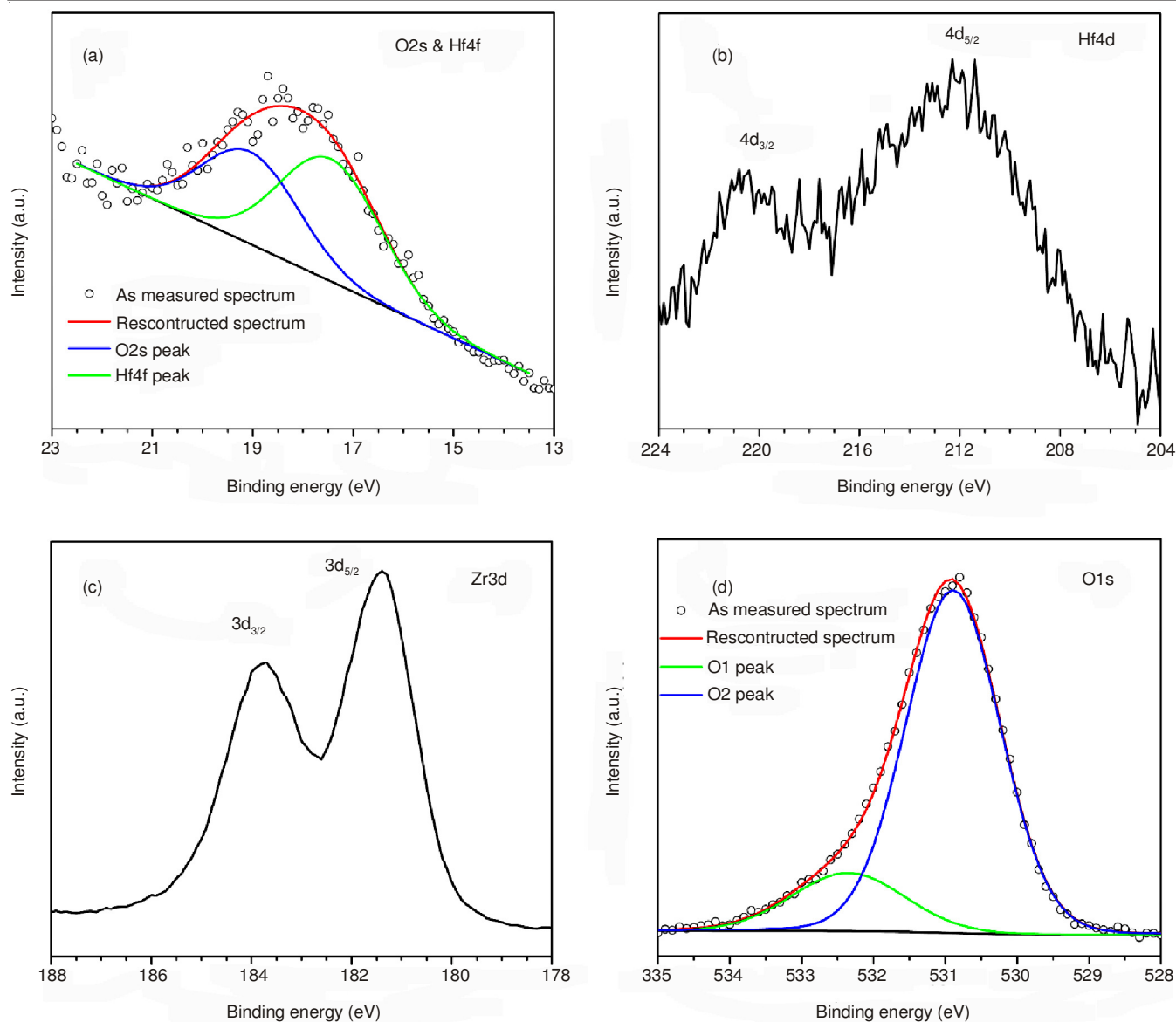


Fig. 2. XPS spectra of the two-step anodized sample (a) O2s and Hf4f with peak fitting, (b) Hf4d, (c) Zr3d and (d) O1s with peak fitting

(monoclinic  $\text{HfO}_2$ ) in the bottom of Fig. 3, these monoclinic diffraction peaks can be identified as the mixture of monoclinic  $\text{ZrO}_2$  and  $\text{HfO}_2$ . In addition, the peak observed at  $2\theta = 30.2^\circ$  suggests the existence of tetragonal  $\text{ZrO}_2$  according to JCPDS card No. 17-0923. The results show that the phase composition of the annealed nanotube layer is the mixture of monoclinic  $\text{ZrO}_2$  and  $\text{HfO}_2$  with small amount of tetragonal phase  $\text{ZrO}_2$ , which confirms that the fabricated nanotubes are  $\text{ZrO}_2\text{-HfO}_2$  binary oxides.

The above experimental facts demonstrate that the highly ordered  $\text{ZrO}_2\text{-HfO}_2$  binary oxides nanotube arrays can be prepared by two-step electrochemical anodization. As  $\text{ZrO}_2$  and  $\text{HfO}_2$  have solid solution behaviour over the entire composition range<sup>32</sup>, changing the composition of Zr-Hf alloys may obtain the highly ordered nanostructured  $\text{ZrO}_2\text{-HfO}_2$  binary oxides with a broad range of different amount ratios. The fabricating approach proposed here may pave the way for preparing the highly ordered nanotubular oxides with a wide range of composition and functionalities.

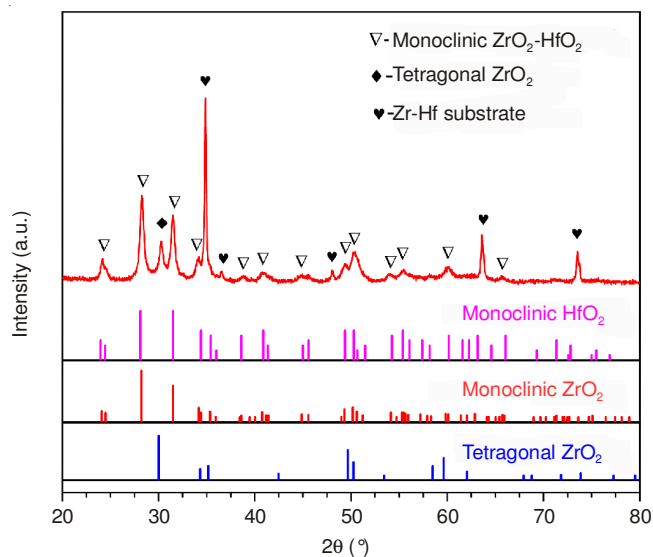


Fig. 3. XRD patterns of the two-step anodized sample after thermal annealing at  $400^\circ\text{C}$  for 3 h

## Conclusion

The highly ordered ZrO<sub>2</sub>-HfO<sub>2</sub> binary oxides nanotube arrays with a length of approximately 6.8 μm, an average diameter of approximate 32 nm and a tube density of 3 × 10<sup>10</sup> cm<sup>-2</sup> were formed by electrochemically anodizing of Zr-Hf alloy in an ethylene glycol electrolyte containing small amounts of fluoride at 30 V with first 0.5 h anodization and second 20 min anodization. The as-formed ZrO<sub>2</sub>-HfO<sub>2</sub> binary oxide nanotube layer was then crystallized *via* a thermal annealing process, after which the mixture of monoclinic ZrO<sub>2</sub> and HfO<sub>2</sub> with small amount of tetragonal phase ZrO<sub>2</sub> were obtained. The fabricating approach developed in the present work inspires to prepare other highly ordered nanotubular oxides with a wide range of composition and functionalities.

## ACKNOWLEDGEMENTS

The authors acknowledged the financial support from the National Natural Science Foundation of China (21373281, 21273293), the Natural Science Foundation of CQ (CSTC2011AB4056), the Program for New Century Excellent Talents in University (NCET-12-0587, NCET-13-0633), the Fundamental Research Funds for the Central Universities (CDJZR13225501, CDJXS12221102), the Program for Excellent Talents in University of Chongqing and the sharing fund of Chongqing University's Large-scale Equipment.

## REFERENCES

1. A.S. Hamdy and M. Farahat, *Surf. Coat. Technol.*, **204**, 2834 (2010).
2. M. Andrieux, P. Ribot, C. Gasquères, B. Servet and G. Garry, *Appl. Surf. Sci.*, **263**, 284 (2012).
3. H.T. Giang, H.T. Duy, P.Q. Ngan, G.H. Thai, D.T. Thu, D.T. Thu and N.N. Toan, *Sens. Actuators B*, **183**, 550 (2013).
4. M. Ghatee, M. Hossain Shariat and J. Irvine, *J. Mater. Chem.*, **18**, 5237 (2008).
5. R. Guttel, M. Paul and F. Schuth, *Chem. Commun.*, **46**, 895 (2010).
6. E. Rossmedgaarden, W. Knowles, T. Kim, M. Wong, W. Zhou, C. Kiely and I. Wachs, *J. Catal.*, **256**, 108 (2008).
7. A. Zydor and S.D. Elliott, *J. Phys. Chem. A*, **114**, 1879 (2010).
8. Z. Fang and D.A. Dixon, *J. Phys. Chem. C*, **117**, 7459 (2013).
9. H.S. Jung, S.A. Lee, S.H. Rha, S.Y. Lee, H.K. Kim, D.H. Kim, K.H. Oh, J.M. Park, W.H. Kim, M.W. Song, N.I. Lee and C.S. Hwang, *IEEE Trans. Electron. Dev.*, **58**, 2094 (2011).
10. J. Müller, T.S. Böscke, U. Schröder, M. Reinicke, L. Oberbeck, D. Zhou, W. Weinreich, P. Kücher, M. Lemberger and L. Frey, *Microelectron. Eng.*, **86**, 1818 (2009).
11. A. Salaün, H. Grampeix, J. Buckley, C. Mannequin, C. Vallée, P. Gonon, S. Jeannot, C. Gaumer, M. Gros-Jean and V. Jousseau, *Thin Solid Films*, **525**, 20 (2012).
12. L. Zaraska, G.D. Sulka, J. Szeremeta and M. Jaskula, *Electrochim. Acta*, **55**, 4377 (2010).
13. K. Schwirn, W. Lee, R. Hillebrand, M. Steinhart, K. Nielsch and U. Gösele, *ACS Nano*, **2**, 302 (2008).
14. D. Losic and D. Losic, *Langmuir*, **25**, 5426 (2009).
15. J.M. Macak, M. Zlamal, J. Krysa and P. Schmuki, *Small*, **3**, 300 (2007).
16. L. Li, Z. Zhou, J. Lei, J. He, S. Zhang and F. Pan, *Appl. Surf. Sci.*, **258**, 3647 (2012).
17. L. Li, Z. Zhou, J. Lei, J. He, S. Wu and F. Pan, *Mater. Lett.*, **68**, 290 (2012).
18. T.S. Kang, A.P. Smith, B.E. Taylor and M.F. Durstock, *Nano Lett.*, **9**, 601 (2009).
19. F. Muratore, A. Baron-Wiechec, A. Gholinia, T. Hashimoto, P. Skeldon and G.E. Thompson, *Electrochim. Acta*, **58**, 389 (2011).
20. F. Muratore, A. Baron-Wiechec, T. Hashimoto, P. Skeldon and G.E. Thompson, *Electrochem. Commun.*, **12**, 1727 (2010).
21. S. Ismail, Z.A. Ahmad, A. Berenov and Z. Lockman, *Corros. Sci.*, **53**, 1156 (2011).
22. L. Li, D. Yan, J. Lei, J. He, S. Wu and F. Pan, *Mater. Lett.*, **65**, 1434 (2011).
23. L. Li, D. Yan, J. Lei, Y. He, J. Xu, N. Li and S. Zhang, *Electrochem. Commun.*, **42**, 13 (2014).
24. S. Berger, F. Jakubka and P. Schmuki, *Electrochem. Solid-State Lett.*, **12**, K45 (2009).
25. X. Qiu, J.Y. Howe, M.B. Cardoso, O. Polat, W.T. Heller and M. Parans Paranthaman, *Nanotechnology*, **20**, 455601 (2009).
26. W. Wei, K. Lee, S. Shaw and P. Schmuki, *Chem. Commun.*, **48**, 4244 (2012).
27. J.Z. Ou, R.A. Rani, M.H. Ham, M.R. Field, Y. Zhang, H. Zheng, P. Reece, S. Zhuiykov, S. Sriram, M. Bhaskaran, R.B. Kaner and K. Kalantarzadeh, *ACS Nano*, **6**, 4045 (2012).
28. Y.C. Nah, A. Ghicov, D. Kim and P. Schmuki, *Electrochem. Commun.*, **10**, 1777 (2008).
29. H.A. El-Sayed and V.I. Birss, *Nanoscale*, **2**, 793 (2010).
30. G. He, G.W. Meng, L.D. Zhang and M. Liu, *Appl. Phys. Lett.*, **91**, 232910 (2007).
31. F. Moulder, W.F. Stickle, P.E. Sobol and K.D. Bomben, *Handbook of X-Ray Photoelectron Spectroscopy*, Perkin-Elmer, Eden Prairie, MN (1991).
32. T.B. Massalski, H. Okamoto, P.R. Subramanian and L. Kacprzak, *Binary Alloy Phase Diagrams*, ASM International, Metals Park, OH, edn 2 (1996).